Journal of Cerebral Blood Flow and Metabolism
15:216–226 © 1995 The International Society of Cerebral Blood Flow and Metabolism
Published by Raven Press, Ltd., New York

Regional Differences in Late-Onset Iron Deposition, Ferritin, Transferrin, Astrocyte Proliferation, and Microglial Activation After Transient Forebrain Ischemia in Rat Brain

*†Yoichi Kondo, *Norio Ogawa, *Masato Asanuma, †Zensuke Ota, and *Akitane Mori

**Department of Neuroscience, Institute of Molecular and Cellular Medicine, and †Third Department of Internal Medicine, Okayama University Medical School, Okayama, Japan*

Summary: With use of iron histochemistry and immunohistochemistry, regional changes in the appearance of iron, ferritin, transferrin, glial fibrillary acidic protein–positive astrocytes, and activated microglia were examined from 1 to 24 weeks after transient forebrain ischemia (four-vessel occlusion model) in rat brain. Expression of the C3bi receptor and the major histocompatibility complex class II antigen was used to identify microglia. Neuronal death was confirmed by hematoxylin–eosin staining only in pyramidal cells of the hippocampal CA_1 region, which is known as the area most vulnerable to ischemia. Perls' reaction with 3,3′-diaminobenzidine intensification revealed iron deposits in the CA_1 region after week 4, which gradually increased and formed clusters by week 24. Iron also deposited in layers III–V of the parietal cortex after week 8 and gradually built up as granular deposits in the cytoplasm of pyramidal cells in frontocortical layer V. An increasing astroglial reaction and the appearance of ferritin-immunopositive microglia paralleled the iron accumulation in the hippocampal CA_1 region, indicating that iron deposition was probably produced in the process of gliosis. Neither neuronal death nor atrophy was found in the cerebral cortex. Nevertheless, an astroglial and ferritin-immunopositive microglial reaction became evident at week 8 in the parietal cortex. On the other hand, the granular iron deposition in the pyramidal neurons of frontocortical layer V was not accompanied by any glial reaction in the chronic stage of ischemia. Three different types of iron deposition in the chronic phase after transient forebrain ischemia were shown in this study. In view of the neuronal damage caused by iron-catalyzed free radical formation, the late-onset iron deposition may be relevant to the pathogenesis of the chronic brain dysfunction seen at a late stage after cerebral ischemia. **Key Words:** Astrocytes—Cerebral ischemia—Cortex—Ferritin—Hippocampus—Immunohistochemistry—Iron—Microglia.

There is increasing interest in brain iron metabolism because abnormal iron deposition in various brain regions has been reported in some neurodegenerative disorders such as Alzheimer disease (Goodman, 1953; Hallgren and Sourander, 1960; Connor et al., 1992), Parkinson disease (Earle, 1968; Dexter et al., 1987; Sofic et al., 1991), amyotrophic lateral sclerosis (Ishikawa et al., 1993), and multiple sclerosis (Craelius et al., 1982; Walton and Kaufmann, 1984).

Iron in various organs is involved in the formation of free radicals, thus contributing to lipid peroxidation (Mead, 1976). It has been said that recirculation of blood after transient cerebral ischemia causes an increase in low molecular weight species of iron (Krause et al., 1987) and that free radical formation initiated by iron ions leads to brain damage by lipid peroxidation (Watson et al., 1984; Komara et al., 1986; Siesjö, 1988).

Despite many studies concerned with a role of iron in neuronal damage during early stages of cerebral ischemia (White et al., 1984, 1985; Babbs, 1985; Rosenthal et al., 1992), abnormal iron deposition at a late stage after transient cerebral isch-

Received March 28, 1994; final revision received August 31, 1994; accepted August 31, 1994.

Address correspondence and reprint requests to Dr. Y. Kondo at Department of Neuroscience, Institute of Molecular and Cellular Medicine, Okayama University Medical School, 2-5-1 Shikatacho, Okayama 700, Japan.

Abbreviations used: DAB, 3,3′-diaminobenzidine; GFAP, glial fibrillary acidic protein; MHC, major histocompatibility complex; PB, phosphate buffer; PBS, phosphate-buffered saline.

emia has not yet been reported except in some cases of children who underwent a severe anoxic–ischemic insult. In these children, iron accumulation was found in the basal ganglia, thalami, and white matter (Dietrich and Bradley, 1988).

In the four-vessel occlusion model in rats (Pulsinelli and Brierley, 1979), which produces a severe transient forebrain ischemia, pyramidal cell death is seen in the selectively vulnerable CA_1 area of the hippocampus 2–3 days after the ischemic period. This delayed neuronal death has been described in both the four-vessel occlusion model in rats (Kirino et al., 1984; Petito and Pulsinelli, 1984) and the 5-min bilateral common carotid artery occlusion model in Mongolian gerbils (Ito et al., 1975; Kirino, 1982; Kirino and Sano, 1984). The ischemic time period in the four-vessel occlusion model varies from 10 to 30 min. It takes 10–20 min of ischemia for delayed neuronal death to develop in the hippocampal CA_1 pyramidal cells, while some striatal neurons are injured immediately after 30 min (Pulsinelli and Brierley, 1979; Pulsinelli et al., 1982*a*). Even 30 min of ischemia does not produce consistent neocortical injury (Ginsberg and Busto, 1989). Several studies have shown that soon after the ischemic insult, damaged brain regions show prominent astrocytosis revealed by immunostaining for glial fibrillary acidic protein (GFAP) (Petito et al., 1990; Schmidt and Szymas, 1990), as well as a microglial reaction. The latter is revealed by the expression of various molecules such as the C3bi complement receptor, major histocompatibility complex (MHC) class I and II glycoproteins, and the CD4 antigen (Gehrmann et al., 1992; Morioka et al., 1992). Little, however, is known about these glial reactions in the long term.

To elucidate iron-related pathology in the brain during the chronic phase after ischemia, we investigated histochemically the spatial and temporal distribution of iron, ferritin, and transferrin (as iron binding proteins), as well as the astroglial and microglial reactions at 1–24 weeks after transient forebrain ischemia produced using the four-vessel occlusion model.

MATERIALS AND METHODS

Experimental animals

Male Wistar rats (Charles River, Yokohama, Japan) weighing 300–360 g (9–10 weeks of age) were used for this study. The method of producing ischemia was the four-vessel occlusion model of Pulsinelli and Brierley (1979). Under sodium pentobarbital (50 mg/kg body wt i.p.) anesthesia, both common carotid arteries were exposed through a ventral midline cervical incision. A silk thread was loosely placed around each artery without interrupting carotid blood flow, and the incision was closed with a single suture. A second incision was made in the dorsal midline of the neck, and both vertebral arteries were electrocauterized with a monopolar coagulator through the alar foramen of the first cervical vertebra. On the next day, under light ether anesthesia, both common carotid arteries were reexposed and occluded with aneurysmal clips to induce forebrain ischemia. At the end of 30 min of bilateral carotid occlusion, blood flow was restored by releasing the clips. Rats that became unresponsive and lost the righting reflex during bilateral carotid artery occlusion and that showed no seizure during and after ischemia were used for the experiment. Only such animals are considered to have met the criteria for adequate ischemia (Pulsinelli et al., 1982*b*).

Sham-operated controls (n = 4 at each time point) were treated similarly to the ischemic group, but neither of the common carotid arteries was occluded. Nonoperated control rats were also studied (n = 2).

Tissue preparation

At 1, 2, 4, 8, and 24 weeks following transient forebrain ischemia, the animals (n = 6 at each time point) were deeply anesthetized with sodium pentobarbital (60 mg/kg body wt i.p.) and then perfusion fixed transcardially with 4% paraformaldehyde in 0.1 *M* phosphate buffer (PB; pH 7.4). The brains were removed and postfixed for ~24 h in the same fixative and cryoprotected, first in 15% sucrose in 0.1 *M* PB and then in 30% sucrose in 0.1 *M* PB. Brains snap frozen with powdered dry ice were cut coronally on a cryostat at 20 μm, and sections including the hippocampus were mounted onto chrom alum/gelatin-coated slides.

Iron histochemistry

Brain iron was determined by Perls' reaction with or without 3,3′-diaminobenzidine (DAB) intensification. The method of intensification of Perls' reaction was that described by Hill and Switzer (1984). Sections were well rinsed in deionized water for at least 30 min, incubated in Perls' solution (1% HCl/1% potassium ferrocyanide) at room temperature for 30 min, and rinsed in deionized water for 30 min. Sections without DAB intensification were counterstained with neutral red and mounted.

For the intensification of Perls' reaction, sections were incubated 20 min in 0.5% DAB in 0.1 *M* PB and 15 min in the same medium including 0.005% H_2O_2, and the reaction was stopped by rinsing in deionized water for >30 min. Sections were mounted and some were counterstained with methyl green.

Control slides were carried through the DAB intensification without preincubation with Perls' solution. No positive staining was found in any such control slides.

Immunohistochemistry

The following mouse or rabbit antibodies were used for immunohistochemical study: anti-ferritin polyclonal antibody (diluted 1:10; Zymet, San Francisco, CA, U.S.A.); anti-transferrin monoclonal antibody (1:100; Cappel, Durham, NC, U.S.A.); anti-GFAP polyclonal antibody (1:10; Nichirei, Tokyo, Japan); MRC OX-42 monoclonal antibody (1:100; Serotec, Crawley Down, U.K.), recognizing the rat C3bi receptor (Robinson et al., 1986); and MRC OX-6 monoclonal antibody (1:100; Serotec), recognizing the rat MHC class II glycoprotein (McMaster and Williams, 1979).

Sections were first rehydrated, washed in 10 m*M* phos-

phate-buffered saline (PBS; pH 7.2), and then incubated with 0.5% H_2O_2 in 10 m*M* PBS to quench endogenous peroxidase activity. After blocking of nonspecific staining with horse or goat serum (i.e., the same species as that of the secondary biotinylated antibody to be used), sections were incubated overnight at 4°C with one of the primary antibodies diluted with 0.1 *M* PBS containing 1% bovine serum albumin overnight. They were washed in 10 m*M* PBS and then incubated with biotinylated anti-mouse or anti-rabbit secondary antibodies (ABC Kit; Vector Lab, Burlingame, CA, U.S.A.) for 1 h. They were washed again and incubated with avidin biotinylated peroxidase reagent (ABC Kit; Vector Lab) for 1 h. The peroxidation activity was visualized by incubating with 0.05% DAB, 50 m*M* imidazole, and 0.006% H_2O_2 in 50 m*M* Tris buffer (pH 7.6) for 4–9 min. The sections were mounted directly or after counterstaining with 1% methyl green. For immunohistochemical controls, the primary antibodies were replaced by mouse or rabbit IgG at appropriate dilutions. No positive staining was seen in any of these control sections.

Double immunostaining was performed with the anti-GFAP and anti-ferritin antibodies. After staining for GFAP as described, the sections were treated with 0.5% H_2O_2 in 10 m*M* PBS and then stained for ferritin in a similar manner except that 1% nickel ammonium sulfate was added in the DAB reaction.

Morphological analysis

To examine histological change in neurons following transient forebrain ischemia, hematoxylin–eosin staining and Klüver Barrera staining were performed. Atrophic changes in coronal sections were also evaluated (Table 1). The thickness of parietal and frontal cortices was estimated by measuring the length between a randomly selected brain surface and the end of layer VI vertical to that brain surface. The thickness of the hippocampus was taken as the maximum distance between the alveus and the stratum lacunosum moleculare of the hippocampal CA_1 region vertical to the alveus. Measurements were performed on photomicrographs of hematoxylin–eosin–stained sections. Statistical evaluations were carried out using two-way analysis of variance followed by Duncan's post hoc tests.

RESULTS

One week after recirculation, pyramidal neurons in the hippocampal CA_1 region already showed ischemic neuronal death (Fig. 1C and D). The neuronal debris did not disappear completely until 24 weeks after recirculation (Fig. 1E and F). The hippocampus was severely atrophic at 24 weeks, as indicated by measurements of hippocampal thickness (Fig. 1E and F; Table 1). No other region except the hippocampal CA_1 area showed neuronal death or atrophy in hematoxylin–eosin–stained sections up to 24 weeks after recirculation (Table 1).

Iron histochemistry

In the sham-operated control rats, the mediodorsal, medial, and ventral thalamic nuclei were relatively abundant in iron as shown by the positive Perls' DAB reaction. Iron staining was also positive in the parenchyma of the tuber cinereum. The hippocampus showed little such staining, but iron was occasionally present in fine granular deposits in the perikarya and neuronal processes of some pyramidal neurons in layer V and part of layer III of the frontal cortex. These iron-laden neurons were significantly more numerous at 24 weeks than at 1 week after the sham operation (Fig. 2).

At 4, 8, and 24 weeks after recirculation in the ischemic group, the granular iron-laden pyramidal neurons of the frontocortical layer V showed an increase with time and were significantly more numerous than in sham-operated controls (Figs. 2 and 3A and B).

Positive staining by Perls' DAB reaction appeared in the hippocampal CA_1 area (Fig. 4D) and in layers III–V of the parietal cortex by 4 weeks after recirculation and reached maximal levels by 8 weeks (Fig. 4E). The staining was greater in the hippocampal CA_1 region than in the parietal cortex. The iron seemed to be contained mainly in microglia, but was also seen to some extent in neurons and in the parenchyma. At 24 weeks, the number of iron-containing cells was decreased, but several iron-laden clusters could be seen in the pyramidal

TABLE 1. *Regional differences in brain atrophy from 1 to 24 wks after 30 min of transient forebrain ischemia*

	Time (wks) after ischemia				
	1	2	4	8	24
Frontal cortex					
Control (n = 4)	1.540 ± 0.148	1.454 ± 0.014	1.619 ± 0.028	1.558 ± 0.029	1.522 ± 0.199
Ischemia (n = 6)	1.476 ± 0.146	1.725 ± 0.040	1.820 ± 0.035	1.613 ± 0.065	1.495 ± 0.140
Parietal cortex					
Control (n = 4)	1.763 ± 0.058	1.453 ± 0.014	1.929 ± 0.050	1.619 ± 0.087	1.769 ± 0.064
Ischemia (n = 6)	1.671 ± 0.043	1.891 ± 0.061	1.749 ± 0.020	1.763 ± 0.174	1.681 ± 0.152
Hippocampus					
Control (n = 4)	0.664 ± 0.041	0.602 ± 0.096	0.661 ± 0.045	0.728 ± 0.014	0.689 ± 0.065
Ischemia (n = 6)	0.630 ± 0.042	0.615 ± 0.061	0.605 ± 0.014[a]	0.556 ± 0.025[a]	0.275 ± 0.062[b]

Values are means ± SD for distance (mm) from brain surface to cortical layer VI (frontal and parietal cortices) and from alveus to stratum lacunosum moleculare of hippocampal CA_1 (hippocampus). See Materials and Methods.

[a] $p < 0.05$, [b] $p < 0.01$ vs. control (sham-operated) group.

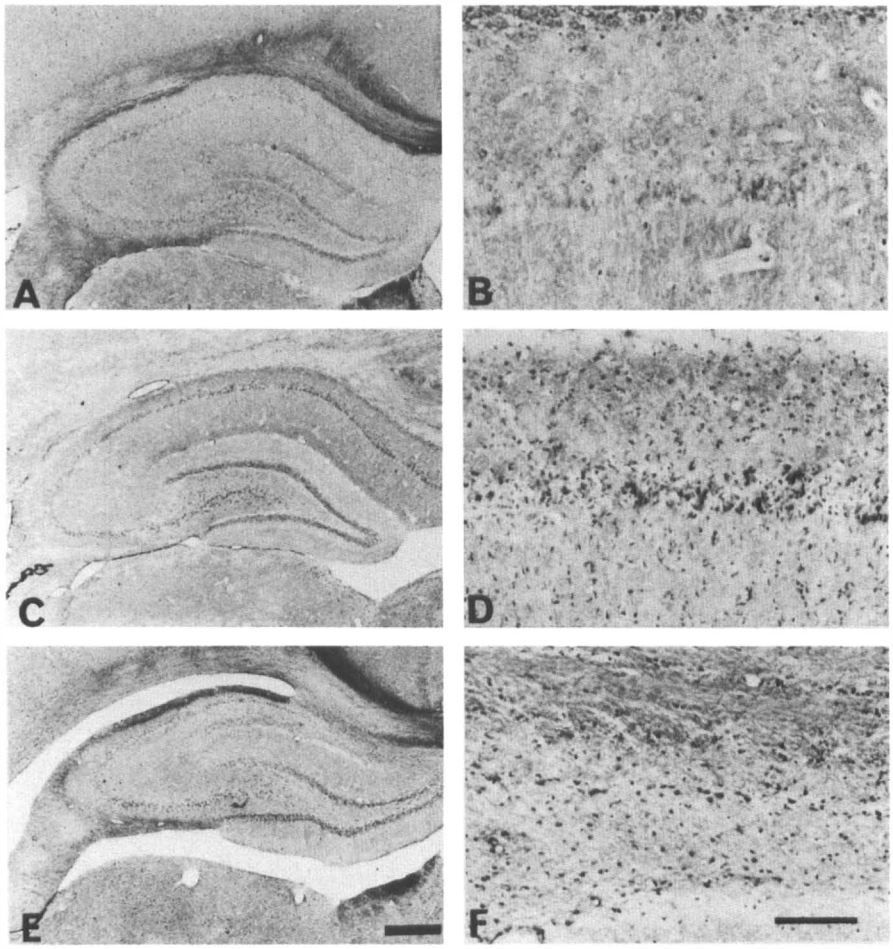

FIG. 1. Photomicrographs of coronal sections at a level of the hippocampus with hematoxylin–eosin staining. Shown are sham-operated control **(A and B)** and ischemic rats at 1 **(C and D)** and 24 **(E and F)** weeks after recirculation. Bar = 500 (A, C, E) and 100 (B, D, F) μm.

cell layer of the hippocampal CA_1 region (Fig. 4F), and a few intensely iron-positive small round cells were found in the parietal cortex.

Of all the iron-containing structures seen using the Perls' reaction with DAB intensification, only the clusters in the hippocampal CA_1 region were positive in the Perls' reaction without DAB. By the nonintensified method, they showed brilliant blue staining, which suggests they contain large amounts of ferric iron.

Ferritin

In the control groups (sham operated and nonoperated), ferritin immunoreactivity was found only to a small extent in the pyramidal layer of the hippocampal CA_1 region (not shown).

At weeks 2 and 4 in the ischemic group, ferritin immunoreactivity was present in the hippocampal CA_1 area (Fig. 5C and D), parietal cortex (Fig. 6C and D), and medial and ventral thalamus, but the staining was not distinct enough to allow identification of the positive structures. At 8 weeks, however, microglia and some neurons in layers III–V of the parietal cortex (Fig. 6E) and microglia in the hippocampal CA_1 area (Fig. 5E) were intensely immunostained for ferritin. By 24 weeks, ferritin immunostaining had decreased notably and only a few positive cells remained (Figs. 5F and 6F), but the

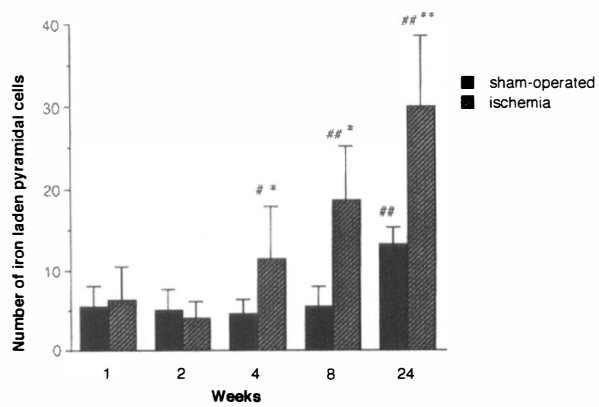

FIG. 2. Number of iron-laden pyramidal neurons in layer V of the frontal cortex. Neurons were counted using a light microscope at a magnification of ×50. An area of 3.0×10^4 μm² (460 μm × 650 μm) of each field in an ocular grid was counted. Values are means ± SD. *$p < 0.05$, **$p < 0.01$ vs. each time-matched sham-operated control. #$p < 0.05$, ##$p < 0.01$ vs. ischemic or sham-operated group at week 1. Two-way analysis of variance followed by Duncan's post hoc test.

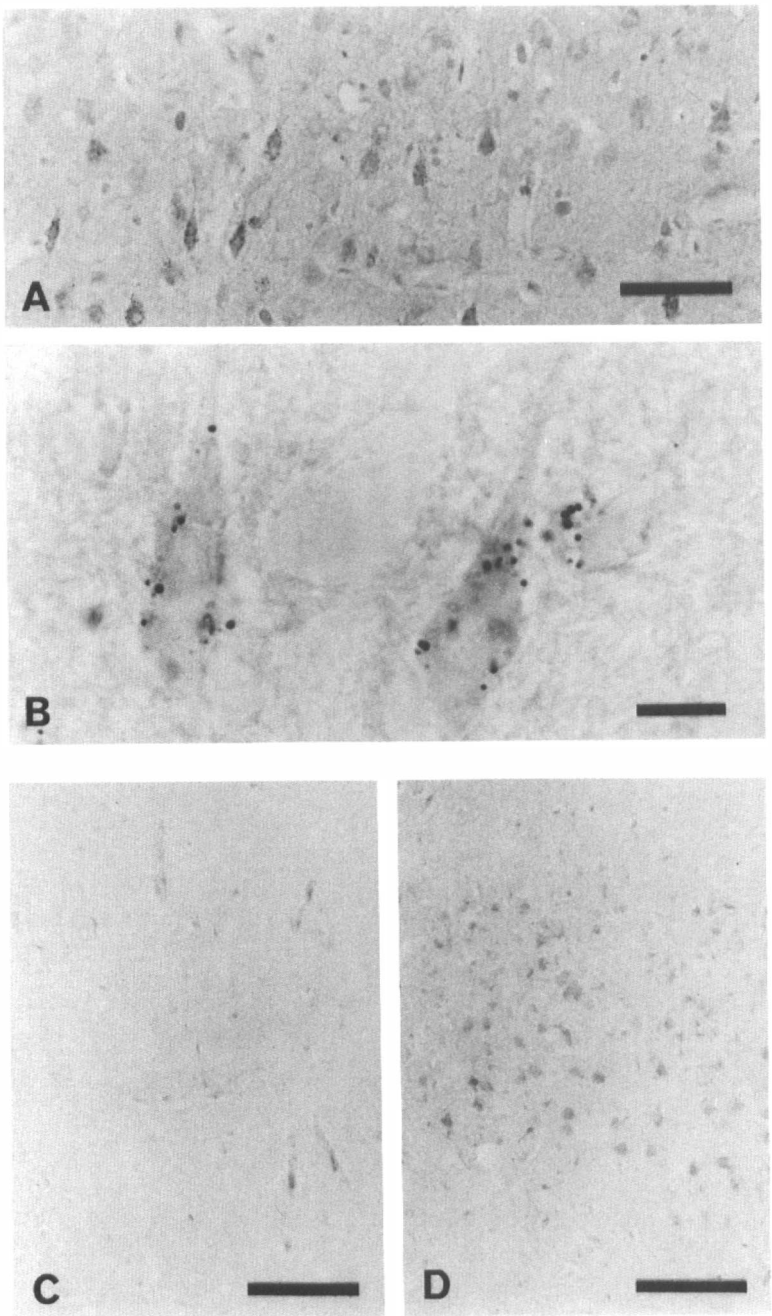

FIG. 3. A and B: Photomicrographs of Perls' iron staining with 3,3′-diaminobenzidine intensification, counterstained with methyl green. Layer V of the frontal cortex is shown at 24 weeks after recirculation (A). The high-power photomicrograph (B) demonstrates granular iron deposition in pyramidal cells of layer V of the frontal cortex 24 weeks after ischemia. **C and D:** Photomicrographs of transferrin immunoreactivity in the parietal cortex. Shown are sham-operated control (C) and 8 weeks after recirculation (D). Bar = 50 (A), 10 (B), and 100 (C, D) μm.

clusters in the pyramidal layer of the hippocampal CA_1 region, which were positive by Perls' reaction, were also strikingly immunoreactive for ferritin.

Transferrin

Transferrin immunoreactivity in the control group was detected only in epithelial cells of choroid plexus and occasionally in perivascular cells (Fig. 3C).

From 2 to 8 weeks after recirculation, neuronal cell bodies in layers III–V in the frontal, parietal, and temporal cortices were immunopositive for transferrin (Fig. 3D). The staining was more intense at week 2 than at later times and had returned to negative by 24 weeks.

GFAP

In the sham-operated control group, GFAP-positive astrocytes were present occasionally in the white matter, subpial area of the cerebral cortex, periventricular area, and hippocampus. These cells were small, with sparse fibrous processes (Figs. 5A and 6A).

One week after recirculation, astrocytes staining densely for GFAP were increased in number in the cerebral cortex (Fig. 6B), hippocampus (Fig. 5B),

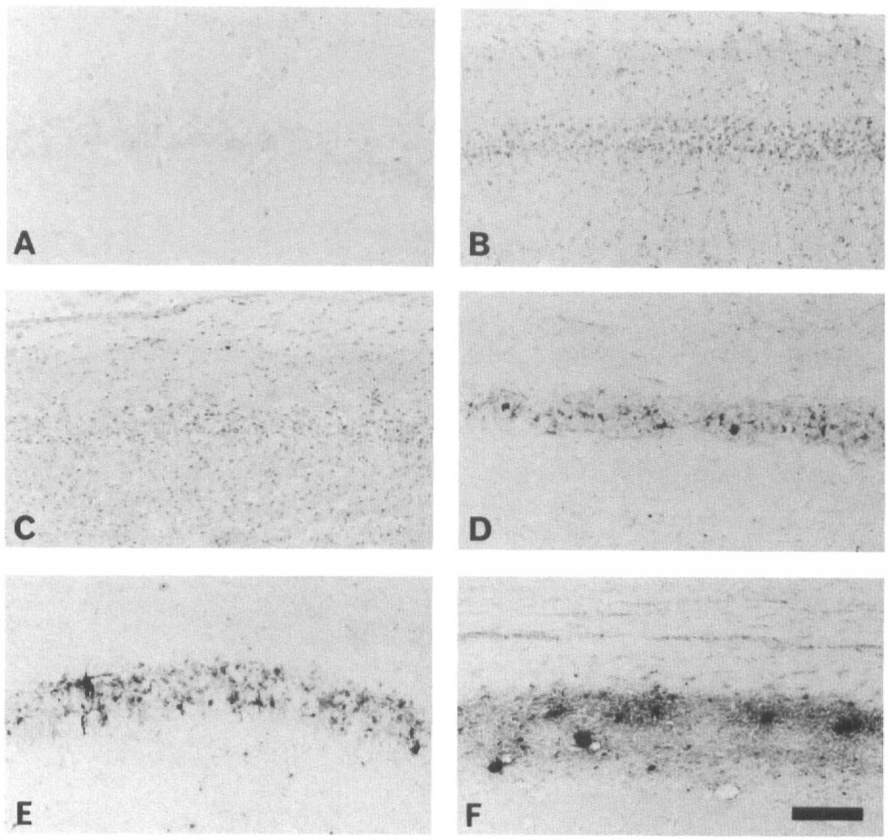

FIG. 4. Photomicrographs of Perls' iron staining with 3,3'-diaminobenzidine intensification in the CA_1 region of the hippocampus, counterstained with methyl green. Shown are sham-operated rats **(A)** and ischemic rats at 1 **(B)**, 2 **(C)**, 4 **(D)**, 8 **(E)**, and 24 **(F)** weeks after recirculation. Bar = 100 μm.

and medial and ventral thalamus (not shown). This increased GFAP immunostaining persisted until the 8th week in the hippocampal CA_1 region (Fig. 5C–E) and in layers III–V of the parietal cortex (Fig. 6C–E), but it had returned to normal levels by the 24th week (Figs. 5F and 6F). Enlargement of the cell bodies and processes of GFAP-positive astrocytes, as well as the increase in numbers, was observed especially in the hippocampal CA_1 area at weeks 2, 4, and 8 (Fig. 5C–E). In the remaining cortical and thalamic areas showing GFAP immunoreactivity at week 2, this staining was decreased at the later time periods.

MRC OX-42 and MRC OX-6

Microglia were immunostained by MRC OX-42 and MRC OX-6. OX-42-positive microglia in the control group were present in the white matter, cerebral cortex (especially in the subpial area), and hippocampus; they had a resting morphology. One week after recirculation, OX-42-positive microglia appeared most remarkably in layers III–V of the frontoparietal cortex (Fig. 7B), the CA_{1-3} regions and dentate gyrus of the hippocampus, and the medial and ventral thalamus. Subsequently, OX-42 immunostaining gradually weakened and returned to normal levels by the 24th week in the parietocortical layers III–V and by the 8th week in the other regions (Fig. 7C and D).

In the control group, only sporadic perivascular cells were immunopositive with OX-6. At weeks 1, 2, and 4, OX-6-positive microglia appeared in the cerebral cortex (Fig. 7F), all hippocampal regions, and the medial and ventral thalamus (not shown). This immunoreactivity had decreased by the 8th week, but was still apparent in layers III–V of the parietal cortex (Fig. 7G), from which, however, it disappeared by week 24 (Fig. 7H).

DISCUSSION

Neuronal death was observed only in the CA_1 region of the hippocampus in our study with the slices at a level of the hippocampus. However, neuronal damage in the middle third of layer III, layers V and VI, or both in the cerebral cortex has also been reported in 30-min period of ischemia produced by four-vessel occlusion (Pulsinelli et al., 1982*a*). This discrepancy may result from the fact that rats from the same strain but different suppliers, or different shipments of rats from the same supplier, vary in their response to four-vessel occlusion (Pulsinelli and Buchan, 1988).

Patterns of iron deposition varied in the different

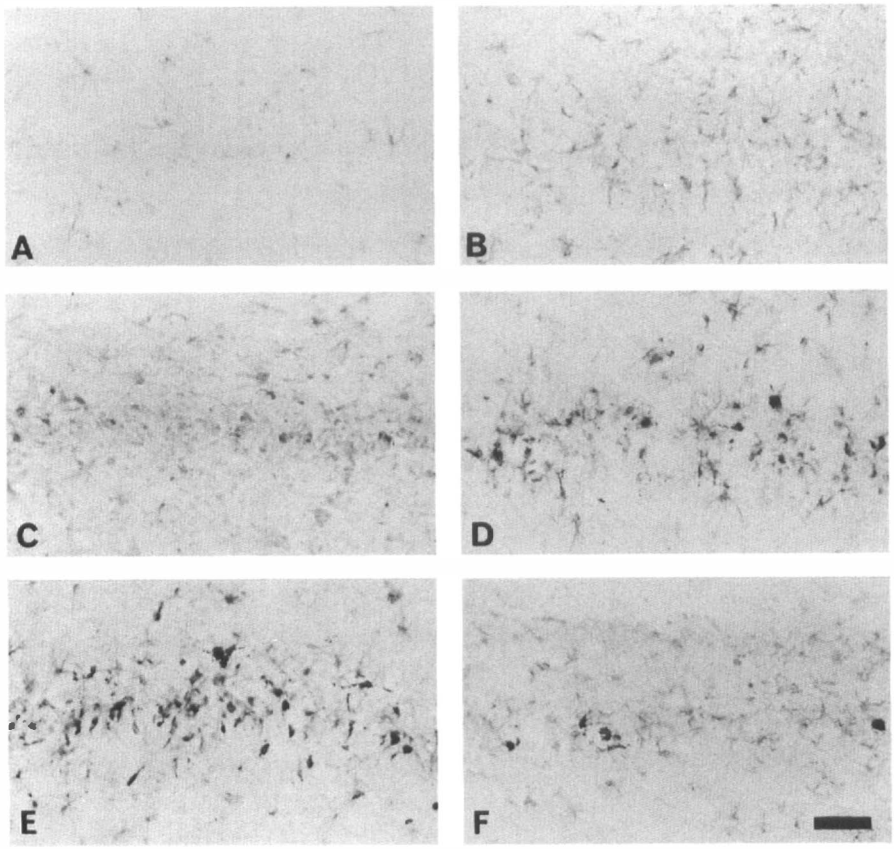

FIG. 5. Double-labeled immunohistochemical preparations of CA_1 of the hippocampus. Glial fibrillary acidic protein–positive astrocytes are brown on the original slides (gray in the photographs), and ferritin-positive cells (predominantly microglia) are dark blue (black in the photographs). Counterstained with methyl green. Shown are sham-operated control **(A)** and ischemic rats at 1 **(B)**, 2 **(C)**, 4 **(D)**, 8 **(E)**, and 24 **(F)** weeks after recirculation. Bar = 50 μm.

brain regions studied, i.e., the hippocampus, parietal cortex, and frontal cortex (Table 2).

In the hippocampal CA_1 area, which is the region most vulnerable to ischemia, iron began to accumulate by 4 weeks after recirculation (Fig. 4D), simultaneously with an increase in the number of GFAP-positive astrocytes and advent of OX-42- and OX-6-positive microglia. Prominent iron deposition was seen at 8 weeks (Fig. 4E), when ferritin immunoreactivity also became apparent, mainly in microglia (Fig. 5E), and GFAP-positive astrocytes showed hypertrophy and stout processes (Fig. 5C–E). By 24 weeks, the glial reactions had subsided (Fig. 5F) and only several clusters positive by Perls' staining (Fig. 4F) remained in the hippocampus showing very marked atrophy (Fig. 1E and F; Table 1). As this time course accords with that described for gliosis, some association may exist between gliosis and disposal of the iron arising from ischemic cell death.

In the parietocortical layers III–V, iron deposition occurred from 4 to 8 weeks after recirculation. The accompanying astroglial and microglial activation was similar to that in the CA_1 region of the hippocampus, but neither neuronal death nor tissue atrophy was found at the light microscopic level (Table 1). The possibility exists that the neurons are, however, functionally disturbed because of the lipid peroxidation that can take place when excessive iron is present to generate free radicals.

In the frontal cortex, some pyramidal cells in layer V had granular iron deposits in their cytoplasm (Fig. 3A and B), and the number of such cells was increased by ischemic insult and with time postischemia (Fig. 2). Interestingly, however, there was not only no tissue injury or atrophy seen in the frontal cortex at the light microscopic level, but there was no glial reaction during the chronic stage after transient ischemia (8–24 weeks after recirculation). This granular iron is almost certainly intrinsic because it also existed in sham-operated and nonoperated control animals, but why it was strikingly increased by ischemia remains unclear. Some pyramidal cell function involving iron metabolism may be compromised by ischemic insult. This granular iron was immunonegative for ferritin, but the form in which it exists remains to be determined.

The iron depositions of the three types described, i.e., that in the hippocampus, parietal cortex, and frontal cortex, were so different as to the forms of iron, the time course, and the extent of glial activation that possible mechanisms of iron-mediated neuronal injury should be considered on a regional basis (Table 2).

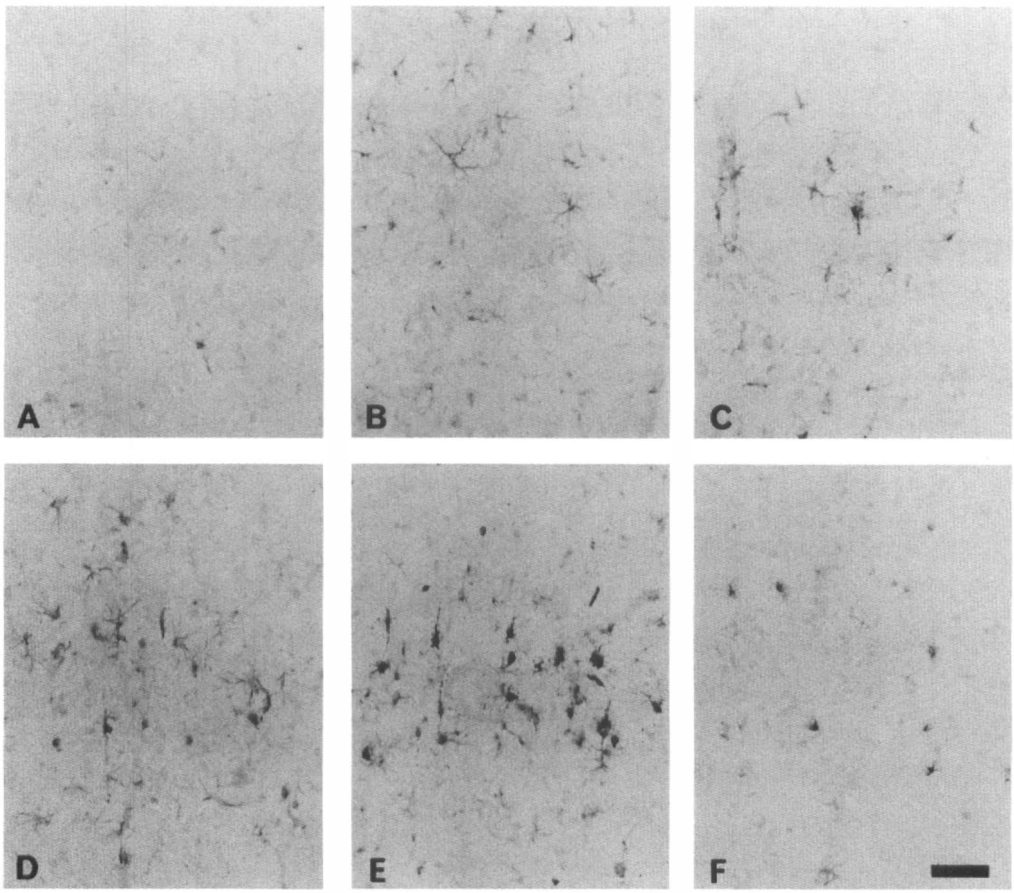

FIG. 6. Double-labeled immunohistochemical preparations of the parietal cortex. Glial fibrillary acidic protein–positive astrocytes are brown on the original slides (gray in the photographs), and ferritin-positive cells (predominantly microglia) are dark blue (black in the photographs). Counterstained with methyl green. Shown are sham-operated control **(A)** and ischemic rats at 1 **(B),** 2 **(C),** 4 **(D),** 8 **(E),** and 24 **(F)** weeks after recirculation. Bar = 50 μm.

Transferrin immunoreactivity was observed widely in neuronal cell bodies of the cerebral cortex from 2 to 8 weeks after recirculation (Fig. 3D). The reason why these neurons were negative by Perls' staining may be that transferrin-bound iron is solubilized in the staining procedure.

Microglia have been reported as an early marker for ischemic neuronal injury (Morioka et al., 1991–1993; Gehrmann et al., 1992), using immunostaining for immune system–related molecules such as the complement receptor, MHC class I and II glycoproteins, and the CD4 antigen. In this study, microglia appeared to be ferritin positive in the hippocampal CA_1 region and in layers III–V of the parietal cortex 8 weeks after recirculation (Figs. 5E and 6E). We suggest that ferritin-immunopositive microglia may be useful as a marker to detect chronic neuronal damage.

There are several possible sources of iron deposition in the ischemic brain. Iron commonly exists in the CNS (Youdim, 1985; Yehuda and Youdim, 1988). In this study, iron accumulated most prominently in the hippocampal CA_1 area where neuronal death was severe, suggesting that the iron originated from neuronal tissue degraded by the ischemic insult. Iron is said to be constantly absorbed from peripheral blood into the brain (Connor and Benkovic, 1992; Roberts et al., 1992). The transferrin immunoreactivity in the epithelial cells of the choroid plexus and in the perivascular cells in normal control rats indicates continuous iron uptake into the brain from both the cerebrospinal fluid and the blood. The functional disturbance of neurons, even if not accompanied by cell death, may cause some failure in transporting or utilizing iron, which could lead to its accumulation in brain regions such as the parietal or frontal cortices. It has been reported that the blood–brain barrier is weakened on exposure to cerebral ischemia (Preston et al., 1993), and this provokes extravasation of plasma protein into the CNS (Schmidt et al., 1990; Nordborg et ál., 1991). It is possible that excess iron migrates to the CNS during ischemia. Krause et al. (1987) reported that the level of low molecular weight species iron,

which might be a prerequisite for lipid peroxidation, was strikingly increased in the brain early in recirculation after transient ischemia. This form of iron returned to normal 8 h after recirculation, although the mechanism is not clear. The possibility exists that low molecular weight species iron was distributed in a pattern similar to that found in this study for excessive iron. Impairment of microvascular perfusion and endothelial cell injury after cerebral ischemia has been reported (Crowell and Olsson, 1972; Ginsberg and Myers, 1972; Hallenbeck and Dutka, 1990), so that some iron in brain may be from hemin iron of disrupted red blood cells in the injured microvessels.

In our recent study on this ischemia model, changes in levels of malondialdehyde and 4-hydroxyalkenals as major decomposition products of lipid peroxidation (Esterbauer and Cheeseman, 1990) were measured spectrophotometrically at 586 nm (the LPO 586 method; Bioxytech S.A., Bonneuil sur Marne, France) on tissue homogenates from the cerebral cortex and hippocampus. The level of lipid peroxidation was significantly increased in the cerebral cortex (162.0% of controls)

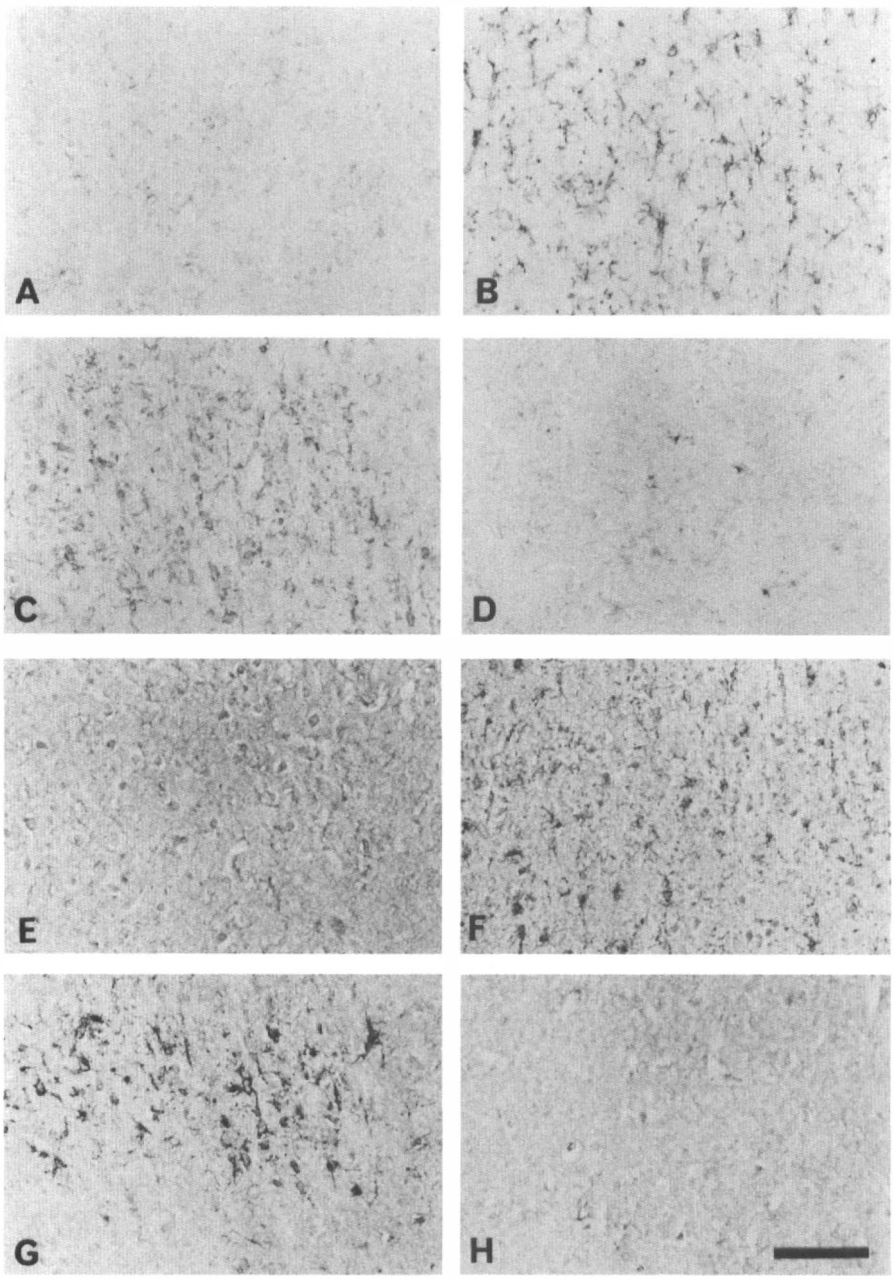

FIG. 7. Immunohistochemical demonstration of MRC OX-42- or MRC OX-6-positive microglia in the parietal cortex without counterstaining. Shown are sham-operated control **(A)** and ischemic rats at 1 **(B)**, 8 **(C)**, and 24 **(D)** weeks after recirculation in MRC OX-42 immunostaining; and sham-operated control **(E)** and ischemic rats at 2 **(F)**, 8 **(G)**, and 24 **(H)** weeks after recirculation in MRC OX-6 immunostaining. Bar = 100 μm.

TABLE 2. *Summary for spatial distribution of iron, its binding proteins, and glial reactions at chronic stage (8 wks after recirculation) of ischemia*

	Brain region		
	Hippocampus	Parietal cortex	Frontal cortex
Iron			
Perls' staining	+ + + +	+ + +	+ +
Ferritin	+ + +	+ +	−
Transferrin	−	+	±
Glia			
Astrocyte (GFAP)	+ +	+ +	−
Microglia (OX-42 and -6)	+ +	+ +	−
Neuronal death	+	−	−

GFAP, glial fibrillary acidic protein.

and in the hippocampus (170.7% of controls) at 24 weeks after recirculation (data not shown), suggesting that neuronal damage caused by lipid peroxidation can occur late after the ischemic insult and that accumulation or disposal of deposited iron is involved in this. By the way, protective agents against an earlier stage of cerebral ischemia previously reported, such as barbiturates (Hallmayer et al., 1985; Kirino et al., 1986) and hypothermia (Busto et al., 1989; Welsh et al., 1990), may certainly prevent iron deposition and resulting neuronal damage. However, in view of preventing this late-onset lipid peroxidation, it is especially interesting to note whether iron chelators or free radical scavengers could be of therapeutic benefit. Iron chelators such as deferoxamine (Komara et al., 1986; Kompala et al., 1986; Rosenthal et al., 1992) may obliterate the iron deposition and prohibit the following late-onset neuronal damage. Moreover, free radical scavengers such as the 21-aminosteroid U74006F (Hall et al., 1988) and the inhibitor of enzymes in the arachidonic acid cascade LY17802 (Clemens et al., 1991) may also be protective without affecting the iron deposition because they scavenge deleterious products of iron deposition. Further work is in progress with these pharmacologies to elucidate the mechanistic associations between the iron deposition and neuronal damage.

Regardless of the sources or mechanisms, deposited iron may lead to lipid peroxidation in neurons and consequent slowly progressive neuronal dysfunction. An iron imbalance has been found as part of the pathophysiology or pathogenesis of a number of neurodegenerative disorders, including Alzheimer disease (Goodman, 1953; Hallgren and Sourander, 1960; Connor et al., 1992) and Parkinson disease (Earle, 1968; Dexter et al., 1987; Sofic et al., 1991). Most work on cerebral ischemia has been focused on the acute stage. It seems possible, however, that the long-term pathological changes accompanied by iron deposition after a transient ischemic insult may be very useful as a new model of chronic neuronal damage.

Acknowledgment: This work was supported in part by Grants-in-Aid for Scientific Research on Priority Areas and Scientific Research from the Japanese Ministry of Education, Science and Culture and by Grants for Research Projects on Aging and Health and for the Research Committee of CNS Degenerative Diseases from the Japanese Ministry of Health and Welfare. The authors thank Prof. Edith G. McGeer, Kinsmen Laboratory of Neurological Research, University of British Columbia, Canada, for criticism of the manuscript.

REFERENCES

Babbs CF (1985) Role of iron ions in the genesis of reperfusion injury following successful cardiopulmonary resuscitation: preliminary data and a biochemical hypothesis. *Ann Emerg Med* 14:777–783

Busto R, Dietrich WD, Globus MY-T, Ginsberg MD (1989) Postischemic moderate hypothermia inhibits CA1 hippocampal ischemic neuronal injury. *Neurosci Lett* 101:299–304

Clemens JA, Ho PPK, Panetta JA (1991) LY178002 reduces rat brain damage after transient global forebrain ischemia. *Stroke* 22:1048–1052

Connor JR, Benkovic SA (1992) Iron regulation in the brain: histochemical, biochemical, and molecular considerations. *Ann Neurol* 32(suppl):51–61

Connor JR, Menzies SL, St. Martin SM, Mufson EJ (1992) A histochemical study of iron, transferrin, and ferritin in Alzheimer's diseased brains. *J Neurosci Res* 31:75–83

Craelius W, Migdal MW, Luessenhop CP, Sugar A, Mihalakis I (1982) Iron deposits surrounding multiple sclerosis plaques. *Arch Pathol Lab Med* 106:397–399

Crowell RM, Olsson Y (1972) Impaired microvascular filling after focal cerebral ischemia in monkeys. *J Neurosurg* 36:303–309

Dexter DT, Wells FR, Agid F, Agid Y, Lees AJ, Jenner P, Marsden CD (1987) Increased nigral iron content in postmortem Parkinsonian brain [Letter]. *Lancet* 2:1219–1220

Dietrich RB, Bradley WJ (1988) Iron accumulation in the basal ganglia following severe ischemic-anoxic insults in children. *Radiology* 168:203–206

Earle KM (1968) Studies in Parkinson's disease including x-ray fluorescent spectroscopy of formalin fixed tissue. *J Neuropathol Exp Neurol* 27:1–14

Esterbauer H, Cheeseman KH (1990) Determination of aldehydic lipid peroxidation products: malonaldehyde and 4-hydroxynonenal. *Methods Enzymol* 186:407–421

Gehrmann J, Bonnekoh P, Miyazawa T, Hossmann K-A, Kreutzburg GW (1992) Immunocytochemical study of an early microglial activation in ischemia. *J Cereb Blood Flow Metab* 12:257–269

Ginsberg MD, Busto R (1989) Rodent models of cerebral ischemia. *Stroke* 20:1627–1642

Ginsberg MD, Myers RE (1972) The topography of impaired microvascular perfusion in the primate brain following total circulatory arrest. *Neurology* 22:998–1011

Goodman L (1953) Alzheimer's disease: a clinicopathologic analysis of twenty-three cases with a theory on pathogenesis. *J Nerv Ment Dis* 118:97–130

Hall ED, Pazara KE, Braughler JM (1988) 21-Aminosteroid lipid peroxidation inhibitor U 74006F protects against cerebral ischemia in gerbils. *Stroke* 19:997–1002

Hallenbeck JM, Dutka AJ (1990) Background review and current concepts of reperfusion injury. *Arch Neurol* 47:1245–1254

Hallgren B, Sourander P (1960) The non-haemin iron in the ce-

rebral cortex in Alzheimer's disease. *J Neurochem* 5:307–310

Hallmayer J, Hossmann K-A, Mies G (1985) Low dose of barbiturates for prevention of hippocampal lesions after brief ischemic episodes. *Acta Neuropathol (Berl)* 68:27–31

Hill JM, Switzer RC (1984) The regional distribution and cellular localization of iron in the rat brain. *Neuroscience* 11:595–603

Ishikawa K, Nagura H, Yokota T, Yamanouchi H (1993) Signal loss in the motor cortex on magnetic resonance images in amyotrophic lateral sclerosis. *Ann Neurol* 33:218–222

Ito U, Spatz M, JT W, Klatzo I (1975) Experimental cerebral ischemia in Mongolian gerbils. I. Light microscopic observations. *Acta Neuropathol (Berl)* 32:209–223

Kirino T (1982) Delayed neuronal death in the gerbil hippocampus following transient ischemia. *Brain Res* 239:57–69

Kirino T, Sano K (1984) Selective vulnerability in the gerbil hippocampus following transient ischemia. *Acta Neuropathol (Berl)* 62:201–208

Kirino T, Tamura A, Sano K (1984) Delayed neuronal death in the rat hippocampus following transient forebrain ischemia. *Acta Neuropathol (Berl)* 64:139–147

Kirino T, Tamura A, Sano K (1986) A reversible type of neuronal injury following ischemia in the gerbil hippocampus. *Stroke* 17:455–459

Komara JS, Nayini NR, Bialick HA, Indrieri RJ, Evans AT, Garritano AM, Hoehner TJ, Jacobs WA, Huang RR, Krause GS, White BW, Aust SD. (1986) Brain iron delocalization and lipid peroxidation following cardiac arrest. *Ann Emerg Med* 15:384–389

Kompala SD, Babbs CF, Blaho KE (1986) Effect of deferoxamine on late deaths following CPR in rats. *Ann Emerg Med* 15:405–407

Krause GS, Nayini NR, White BC, Hoenher TJ, Garritano AM, O'Neil BJ, Aust SD (1987) Natural course of iron delocalization and lipid peroxidation during the first eight hours following a 15-minute cardiac arrest in dogs. *Ann Emerg Med* 16:1200–1205

McMaster WR, Williams AF (1979) Identification of la glycoproteins in rat thymus and purification from rat spleen. *Eur J Immunol* 9:426–433

Mead JF (1976) Free radical mechanisms of lipid damage and consequences for cellular membranes. In: *Free Radicals in Biology* (Pryor WA, ed), New York, Academic Press, pp 51–68

Morioka T, Kalehua AN, Streit WJ (1991) The microglial reaction in the rat dorsal hippocampus following transient forebrain ischemia. *J Cereb Blood Flow Metab* 11:966–973

Morioka T, Kalehua AN, Streit WJ (1992) Progressive expression of immunomolecules on microglial cells in rat dorsal hippocampus following transient forebrain ischemia. *Acta Neuropathol (Berl)* 83:149–157

Morioka T, Kalehua AN, Streit WJ (1993) Characterization of microglial reaction after middle cerebral artery occlusion in rat brain. *J Comp Neurol* 327:123–132

Nordborg TE, Sokrab O, Johansson BB (1991) The relationship between plasma protein extravasation and remote tissue changes after experimental brain infarction. *Acta Neuropathol* 82:118–126

Petito CK, Pulsinelli WA (1984) Delayed neuronal recovery and neuronal death in rat hippocampus following severe cerebral ischemia: possible relationship to abnormalities in neuronal processes. *J Cereb Blood Flow Metab* 4:194–205

Petito CK, Morgello S, Felix JC, Lesser ML (1990) The two patterns of reactive astrocytosis in postischemic rat brain. *J Cereb Blood Flow Metab* 10:850–859

Preston E, Sutherland G, Finsten A (1993) Three openings of the blood–brain barrier produced by forebrain ischemia in the rat. *Neurosci Lett* 149:75–78

Pulsinelli WA, Brierley JB (1979) A new model of bilateral hemispheric ischemia in the unanesthetized rat. *Stroke* 10:267–272

Pulsinelli WA, Buchan AM (1988) The four-vessel occlusion rat model: method for complete occlusion of vertebral arteries and control of collateral circulation. *Stroke* 19:913–914

Pulsinelli WA, Brierley JB, Plum F (1982*a*) Temporal profile of neuronal damage in a model of transient forebrain ischemia. *Ann Neurol* 11:491–498

Pulsinelli WA, Levy DE, Duffy TE (1982*b*) Regional cerebral blood flow and glucose metabolism following transient forebrain ischemia. *Ann Neurol* 11:491–499

Roberts R, Sandra A, Siek GC, Lucas JJ, Fine RE (1992) Studies of the mechanism of iron transport across the blood-brain barrier. *Ann Neurol* 32:43–50

Robinson AP, White TM, Mason DW (1986) Macrophage heterogeneity in the rat as delineated by two monoclonal antibodies MRC OX-41 and OX-42, the latter recognizing complement receptor type 3. *Immunology* 57:239–247

Rosenthal RE, Chanderbhan R, Marshall G, Fiskum G (1992) Prevention of post-ischemic brain lipid conjugated diene production and neurological injury by hydroxyethyl starch-conjugated deferoxamine. *Free Radical Biol Med* 12:29–33

Schmidt KR, Szymas J (1990) Immunohistochemistry of glial fibrillary acidic protein, vimentin and S-100 protein for study of astrocytes in hippocampus of rat. *J Chem Neuroanat* 3: 179–192

Schmidt KR, Szymas J, Hossmann K-A (1990) Immunohistochemical study of glial reaction and serum protein extravasation in relation to neuronal damage in rat hippocampus after ischemia. *Neuroscience* 38:527–540

Siesjö BK (1988) Mechanisms of ischemic brain damage. *Crit Care Med* 16:954–963

Sofic E, Paulus W, Jellinger K, Riederer P, Youdim MB (1991) Selective increase of iron in substantia nigra zona compacta of parkinsonian brains. *J Neurochem* 56:978–982

Walton JC, Kaufmann JC (1984) Iron deposits and multiple sclerosis. *Arch Pathol Lab Med* 108:755–756

Watson BD, Busto R, Goldberg WJ (1984) Lipid peroxidation in vivo induced by reversible global ischemia in rat brain. *J Neurochem* 42:268–274

Welsh FA, Sims RE, Harris VA (1990) Mild hypothermia prevents ischemic injury in gerbil hippocampus. *J Cereb Blood Flow Metab* 10:557–563

White BC, Aust SD, Arfors KE, Aronson LD (1984) Brain injury by ischemic anoxia: hypothesis extension—a tale of two ions? *Ann Emerg Med* 13:862–867

White BC, Krause GS, Aust SD, Eyster GE (1985) Postischemic tissue injury by iron-mediated free radical lipid peroxidation. *Ann Emerg Med* 14:804–809

Yehuda S, Youdim MBH (1988) Brain iron deficiency: biochemistry and behavior. In: *Brain Iron: Neurochemical and Behavioural Aspects* (Yehuda S, Youdim MBH, eds), London, Taylor and Francis, pp 89–114

Youdim MBH (1985) Brain iron metabolism. In: *Handbook of Neurochemistry* (Lajtha A, ed), New York, Plenum Press, pp 731–777